In Vivo Imaging of Human Colorectal Cancer Using Radiolabeled Analogs of the Uroguanylin Peptide Hormone

DIJIE LIU[1,5], DOUGLAS OVERBEY[1], LISA D. WATKINSON[1,5], SAID DAIBES-FIGUEROA[1,5],
TIMOTHY J. HOFFMAN[1,4,5], LEONARD R. FORTE[1,3,5], WYNN A. VOLKERT[1,2,5] and MICHAEL F. GIBLIN[1,2,5,*]

[1]Research Service, Harry S. Truman Memorial Veterans' Administration Hospital, Columbia, MO 65201;
Departments of [2]Radiology, [3]Medical Pharmacology and Physiology, and [4]Internal Medicine, and
[5]The Radiopharmaceutical Sciences Institute, University of Missouri-Columbia, Columbia, MO 65211, U.S.A.

Abstract. *Background: Uroguanylin is an endogenous peptide agonist that binds to the guanylate cyclase C receptor (GC-C). GC-C is overexpressed in human colorectal cancer (CRC), and exposure of GC-C-expressing cells to GC-C agonists results in cell cycle arrest and/or apoptosis, highlighting the therapeutic potential of such compounds. This study describes the first use of radiolabeled uroguanylin analogs for in vivo detection of CRC. Materials and Methods: The peptides uroguanylin and E³-uroguanylin were N-terminally labeled with the DOTA chelating group via NHS ester activation and characterized by RP-HPLC, ESI-MS, and GC-C receptor binding assays. The purified conjugates were radiolabeled with In-111 and used for in vivo biodistribution and SPECT imaging studies. In vivo experiments were carried out using SCID mice bearing T84 human colorectal cancer tumor xenografts. Results: Alteration of the position 3 aspartate residue to glutamate resulted in increased affinity for GC-C, with IC_{50} values of 5.0±0.3 and 9.6±2.9 nM for E^3-uroguanylin and DOTA-E^3-uroguanylin, respectively. In vivo, ^{111}In-DOTA-E^3-uroguanylin demonstrated tumor uptake of 1.17±0.23 and 0.61±0.07% ID/g at 1 and 4 h post injection, respectively. The specificity of tumor localization was demonstrated by co-injection of 3 mg/kg unlabeled E^3-uroguanylin, which reduced tumor uptake by 69%. Uptake in kidney, however, was dramatically higher for the uroguanylin peptides than for previously characterized radiolabeled E. coli heat-stable enterotoxin (STh) analogs targeting GC-C, and was also inhibited by coinjection of unlabeled peptide in a fashion not previously observed. Conclusion: Use of uroguanylin-targeting vectors for in vivo imaging of colorectal cancers expressing GC-C resulted in tumor uptake that paralleled that of higher affinity heat-stable enterotoxin peptides, but also resulted in increased kidney uptake in vivo.*

Correspondence to: Dr. Michael F. Giblin, Harry S. Truman Memorial VA Hospital, Research Service Room A004, 800 Hospital Drive, Columbia, MO 65201, U.S.A. Tel: +1 5738146000 ext. 53669, Fax: +1 5738821663, e-mail: giblinm@health.missouri.edu

Guanylate cyclase C (GC-C) is a type I transmembrane glycoprotein expressed on brush border membranes of intestinal epithelial cells, as well as on transformed human colon cancer cell lines such as the T-84 cell line (1, 2). In the normal intestinal mucosa, GC-C receptors are expressed within the apical (luminal) face of epithelial cell membranes, and are therefore isolated from the bloodstream by cell-cell tight junctions (3-6). GC-C expression is maintained in transformed cells throughout the process of colorectal carcinogenesis, while expression of the endogenous GC-C ligands guanylin and uroguanylin is typically lost (7-9). Normally expressed at high levels within the lumen of the gut, GC-C is expressed on virtually all histologically confirmed primary and metastatic colorectal tumors examined in human patients, while normal tissues and other types of cancer express minimal or no GC-C receptors (4-6). GC-C receptors on colorectal tumors retain their ligand-binding capacity, and expression of GC-C receptors does not vary as a function of metastatic site or grade of these tumors (5). The unique expression of GC-C by metastatic cells of colorectal origin within lymph nodes of patients undergoing staging for colorectal cancer (CRC) forms the basis for a PCR-based diagnostic test that is currently undergoing clinical trials (10). GC-C expression has also formed the basis of development of ligand-based molecular agents for *in vivo* detection and therapy of colorectal cancer (9, 11-20).

Uroguanylin is a 16 amino acid peptide with two disulfide bonds, and has nanomolar affinity for the GC-C receptor (21, 22). Secretion of the endogenous peptides guanylin and uroguanylin into the lumen of the gut by enterochromaffin cells plays a role in regulation of ion and fluid homeostasis

by activation of the cystic fibrosis transmembrane conductance regulator (CFTR), generating net efflux of sodium, chloride, bicarbonate, and water into the lumen of the intestine (23). In nature, the *E. coli* heat-stable enterotoxin (STh) is expressed by enterotoxigenic strains of *E. coli* bacteria in order to co-opt the endogenous uroguanylin/GC-C ligand-receptor system. Bacteria such as *E. coli* have evolved heat-stable peptides which differ structurally from uroguanylin family peptides in that they possess a third disulfide bond, which is presumably responsible for both increased resistance to heat/enzymatic degradation as well as superagonist activity. These guanylin/uroguanylin mimics are also the highest affinity ligands known for the GC-C receptor (22, 23).

We have developed numerous analogs of the *E. coli* heat-stable enterotoxin for the purpose of developing an optimal molecular imaging vector for colorectal cancer (11, 13-15). Such imaging constructs could enable noninvasive imaging of CRC patients, and help to define patient groups that could benefit from treatment with GC-C agonists. Here, we examine the consequences of using the structurally less complex uroguanylin molecule on targeting efficiency. *In vivo* targeting was assessed using peptides with N-terminal DOTA macrocyclic chelators, labeled with the radionuclide In-111. Two analogs of the uroguanylin peptide have been compared with respect to *in vitro* binding affinity and *in vivo* biodistribution patterns in SCID mice bearing T84 human colorectal cancer tumor xenografts.

Materials and Methods

All solvents were either ACS certified or HPLC grade solvents obtained from Fischer Scientific and used as received. DOTA-NHS ester was purchased from Macrocyclics (Dallas, TX, USA). $^{111}InCl_3$ was obtained from Mallinckrodt Medical, Inc (St. Louis, MO, USA) as a 0.05 N HCl solution. Wild-type human uroguanylin was obtained from the American Peptide Company, and E^3-uroguanylin was kindly provided by Dr. Kunwar Shailubhai at Callisto Pharmaceuticals. All other reagents were purchased from Aldrich Chemical Company. Human colon carcinoma T-84 cells were obtained from the American Type Culture Collection (ATCC) and maintained and grown for use in these studies in the University of Missouri Cell and Immunology Core facilities. MALDI-TOF mass spectral analyses were performed by the proteomics core facility at the University of Missouri-Columbia.

High performance liquid chromatography (HPLC). High performance liquid chromatography (HPLC) analyses were performed on a Shimadzu system equipped with an SPD-20A UV detector and an in-line sodium iodide crystal radiometric detector. HPLC solvents consisted of H_2O containing 0.1% trifluoroacetic acid (solvent A) and acetonitrile containing 0.1% trifluoroacetic acid (solvent B). Conditions: A Phenomenex Jupiter C-18 (5 μm, 300 Å, 4.6×250 mm) column was used with a flow rate of 1.5 ml/min. Gradient purification of compounds is achieved during a linear 30 minute ramp from 23% B to 33% B, followed by column rinse and re-equilibration.
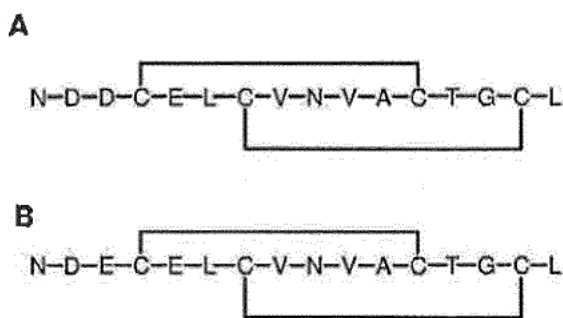
Peptide synthesis and radiolabeling. F19-STh(1-19) was iodinated by a modified lactoperoxidase method. Briefly, 2 μg peptide was suspended in 50 μl 100 mM sodium phosphate buffer, pH 7.5, containing 2 μg lactoperoxidase and 0.25-1.0 mCi Na^{125}I. The reaction was initiated by addition of 2 μl of a 1:10,000 dilution of 30% H_2O_2. The reaction was incubated 30 min at room temperature with occasional mixing, then diluted with dH2O and purified to homogeneity by RP-HPLC.

DOTA labeling of the folded uroguanylin peptides proceeded using a 100-fold molar excess of the DOTA-NHS ester. The reactions were incubated in 150 mM HEPES at 4°C overnight, quenched with TRIS buffer and purified by C18 RP-HPLC. HPLC purified DOTA-peptides were subsequently characterized by ESI-MS and *in vitro* cell binding assay. For the synthesis of ^{111}In-labeled compounds, aliquots of $^{111}InCl_3$ (0.2-2.5 mCi, 4-50 μl) were added to solutions of 50 μg of respective peptides in 0.2 M ammonium acetate (200 μl). The pH of reaction mixtures was adjusted to 5.8, and reactions were incubated for 1 hour at 80°C. After 1 hour, 2 mM EDTA (50 μl) was added to complex unreacted $^{111}In+3$. The resulting conjugates were purified to homogeneity by RP-HPLC. The ^{111}In-metallated conjugates eluted between 1.1-1.9 minutes before the associated non-metallated species enabling collection of high-specific activity, no carrier-added ^{111}In-peptide conjugates. All purified ^{111}In-peptide conjugates were then concentrated by passing through a 3M Empore C-18 HD high performance extraction disk (7 mm/3 ml) cartridge and eluting with 50% ethanol in 0.1 M NaH$_2$PO$_4$ buffer (500 μl). The concentrated fraction was then reduced in volume under a stream of N_2, and finally diluted with 0.1 M NaH$_2$PO$_4$ buffer, pH 7.0, to a final activity of approximately 2 μCi/100 μl.

In vitro cell binding studies. Peptide IC$_{50}$s were determined by a competitive displacement cell binding assay using ^{125}I-F19-ST$_h$(1-19). Briefly 3×10^6 cells suspended in DMEM/F-12 media containing 15 mM MES and 0.2% BSA, were incubated at 37°C for 1 hour in presence of approximately 20,000 cpm ^{125}I-tracer and increasing concentration of the DOTA-peptide conjugates. After the incubation, the reaction medium was aspirated and cells were washed three times with media. The radioactivity bound to the cells was counted in a Packard Riastar gamma counting system. The % ^{125}I-F19-ST$_h$(1-19) bound to cells was plotted *vs.* increasing concentrations of DOTA-peptides to determine the respective IC$_{50}$ values. For statistical considerations, duplicate *in vitro* cell binding experiments with each analog were performed. IC$_{50}$ calculations were performed using the 4 parameter logistic model within the program grafit (Erithacus Software, Ltd).

In vivo pharmacokinetic studies of ^{111}In-peptide analogs in SCID mice. Four- to 5-week old female ICR SCID (severe combined immunodeficient) outbred mice were obtained from Taconic (Germantown, NY). The mice were housed four animals per cage in sterile micro isolator cages in a temperature- and humidity-controlled room with a 12-hour light/12-hour dark schedule. The animals were fed sterile rodent chow (Ralston Purina Company, St. Louis, MO, USA) and water *ad libitum*. Animals were housed one week prior to inoculation of tumor cells and anesthetized for injections with isoflurane (Baxter Healthcare Corp., Deerfield, IL, USA) at a rate of 2.5% with 0.4l oxygen through a non-rebreathing anesthesia vaporizer.

Human colon cancer T-84 cells were injected on the bilateral subcutaneous (s.c.) flank with ~5×10^6 cells in a suspension of 100

A

N–D–D–C–E–L–C–V–N–V–A–C–T–G–C–L

B

N–D–E–C–E–L–C–V–N–V–A–C–T–G–C–L

Figure 1. *Structures of (A) and uroguanylin (B) E^3-uroguanylin.*

Figure 2. *IC_{50} analyses of uroguanylin analog displacement of ^{125}I-F^{19}-STh(1-19) from T84 human colorectal cancer cells.*

Table I. *Calculated and observed $(M+H)^+$ values and IC_{50} values (± SD) for characterized peptides.*

Peptide	$(M+H)^+$ Calc.	$(M+H)^+$ Obs.	IC_{50} (nM)
Uroguanylin	1667.6	1667.7	39.8±14.9
DOTA-uroguanylin	2053.6	2053.9	34.5±3.3
E^3-uroguanylin	1681.6	1681.6	5.0±0.3
DOTA-E^3-uroguanylin	2067.6	2067.9	9.6±2.9

µl 3:1 PBS:Matrigel (BD Biosciences, Bedford, MA, USA) per injection site. T-84 cells were allowed to grow *in vivo* four to six weeks post inoculation, developing tumors ranging in sizes from 0.06-0.59 grams. The biodistribution and uptake of ^{111}In-DOTA-uroguanylin and ^{111}In-DOTA-E^3-uroguanylin in tumor bearing SCID mice was studied following randomization of animals such that no significant ($p<0.05$) differences existed with respect to tumor sizes between test groups. The mice (average weight, 25 g) were injected with aliquots (50-100 µl) of the radiolabeled peptide solution (1-3 µCi) in each animal *via* the tail vein. Tissues, organs and tumors were excised from animals sacrificed at 1 hour and 4 hour post-injection (*p.i.*), weighed, and counted. Radioactivity was measured in a NaI counter and the percent-injected dose per organ and the percent-injected dose per gram tissue were calculated. Animal studies were conducted in accordance with the highest standards of care as outlined in the NIH guide for Care and Use of Laboratory Animals and the Policy and Procedures for Animal Research at the Harry S. Truman Memorial Veterans' Hospital and according to approved protocols.

SPECT/CT imaging. A combined micro-SPECT/CT unit (microCAT II, Siemens Medical Systems) was employed for Single Photon Emitting Computed Tomography/ Computed Tomography imaging studies. One SCID mouse bearing T84 human colorectal cancer tumor xenografts was injected intravenously with 220 µCi (100 µl) ^{111}In-DOTA-uroguanylin solution and sacrificed at 1 hour *p.i.* Micro-SPECT scans of 60 projections were performed using a symmetrical 20% photopeak discriminating window. Volumetric data from SPECT and CT was visualized and image fused using Amira 3.1 (TGS, San Diego, CA, USA).
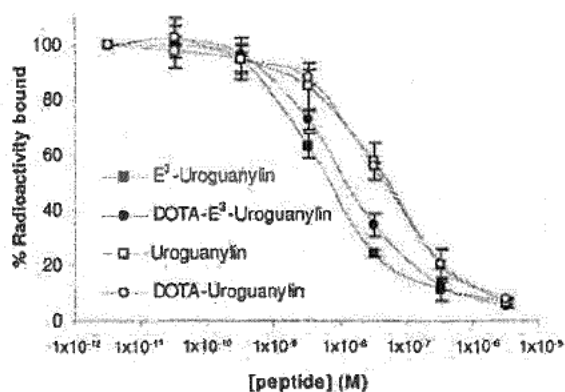
Results

Two DOTA-labeled uroguanylin analogs were synthesized in this work, and their characteristics as agents targeting the GC-C receptor were compared to those of previously synthesized analogs of the *E. coli* heat-stable enterotoxin (STh) (13, 14). Each of these peptides is structurally related, and the two uroguanylin analogs differ only in a conservative D3E substitution (Figure 1). Uroguanylin peptides share significant sequence homology with STh, including absolute conservation of four cysteine residues that form a conserved array of disulfide bonds (Figure 1). Analogs of the *E. coli* heat-stable enterotoxin also possess a third disulfide bond, lending these bacterial uroguanylin mimics exceptional stability and affinity for the GC-C receptor.

Peptides were purified by RP-HPLC and characterized by MALDI-TOF MS and by a competitive displacement receptor binding assay utilizing T84 human colorectal cancer cells and ^{125}I-labeled F^{19}-STh(1-19) (Table I, Figure 2). Observed IC_{50} values for uroguanylin and DOTA-uroguanylin (39.8±14.9 and 34.5±3.3 nM, respectively) were significantly higher than those of previously characterized STh analogs, as expected from previous studies of this class of peptide agonists (13-15, 22). A conservative D3E substitution, however, significantly increased the binding affinities of the resultant uroguanylin analogs, with measured IC_{50} values for E^3-uroguanylin and DOTA-E^3-uroguanylin of 5.0±0.3 and 9.6±2.9 nM, respectively.

To determine the effects of affinity differences on *in vivo* tumor localization, DOTA peptides were labeled with ^{111}In and purified by RP-HPLC (Figure 3). Addition of *N*-terminal DOTA moieties resulted in a 0.9-1.1-minute shift to earlier retention times for each uroguanylin peptide. Further 1.1-1.9-minute shifts to earlier retention times were observed upon coordination of ^{111}In by DOTA peptides. ^{111}In-labeled uroguanylin analogs were
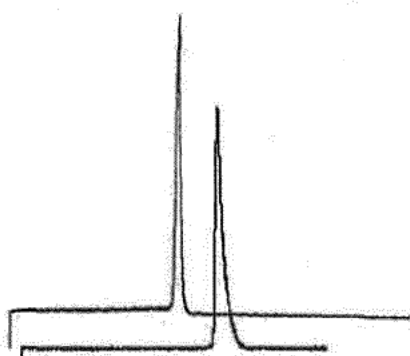
Figure 3. RP-HPLC chromatograms of purified ^{111}In-DOTA-E[3]-uroguanylin (top), ^{111}In-DOTA- uroguanylin (bottom).

Figure 4. Biodistribution analysis of ^{111}In-DOTA-E[3]-uroguanylin with and without co-injection of 70 μg unlabeled E[3]-uroguanylin, and ^{111}In-DOTA-uroguanylin at 1 hr pi (% ID/g, N=4).

found to possess chromatographic properties corresponding to those of previously characterized ^{111}In-labeled STh peptides, requiring similar acetonitrile concentrations for elution from a C18 RP-HPLC column. RP-HPLC purification of each ^{111}In-labeled peptide resulted in high specific activity radiotracers that were subsequently tested in animal models.

In vivo, tumor uptake of ^{111}In-DOTA-E[3]-uroguanylin at 1 hour *p.i.* trended higher than that of ^{111}In-DOTA-uroguanylin (1.04 ± 0.07 and 0.88 ± 0.33 % ID/g, respectively), although the difference did not achieve the $p < 0.05$ significance level (Figure 4). ^{111}In-DOTA-E[3]-uroguanylin demonstrated significant ($p < 0.001$) specific tumor uptake in T84 human colorectal cancer tumor xenografts, as uptake of this compound was reduced to 0.32 ± 0.06 % ID/g at 1 hour *p.i.* by co-injection of saturating concentrations of unlabeled E[3]-uroguanylin (Figure 4). Uptake in tumor at 1 hour *p.i.* was higher than for all other tissues, with the exception of kidney. Tumor/blood, tumor/muscle, and tumor/liver ratios at this timepoint were 4.7, 20.8, and 6.1, respectively. At 4 hours *p.i.*, tumor uptake of ^{111}In-DOTA-E[3]-uroguanylin decreased to 0.61 ± 0.07 % ID/g. However, activity also rapidly washed out of nontarget tissues, resulting in tumor/blood, tumor/muscle, and tumor/liver ratios of 61, 61, and 4.4, respectively at 4 hours *p.i.* These target:nontarget ratios compare favorably in certain respects with those obtained previously at the same time *p.i.* using STh peptides such as ^{111}In-DOTA-R[1,4],F[19]-STh(1-19) (21, 55, and 4.4, respectively) (13), although tumor uptake was generally higher for ^{111}In-DOTA-labeled STh peptides (1.64 % ID/g at 4 hour *p.i.* for ^{111}In-DOTA-R[1,4],F[19]-STh(1-19)) (13, 14).

The most significant difference between the *in vivo* biodistribution of uroguanylin analogs and previously characterized STh peptides related to uptake in kidney. While the observed kidney uptake of ^{111}In-DOTA-labeled STh analogs at 4 hours *p.i.* has previously been observed in the range of 2.2-4.3 % ID/g (13-15), ^{111}In-DOTA-E[3]-
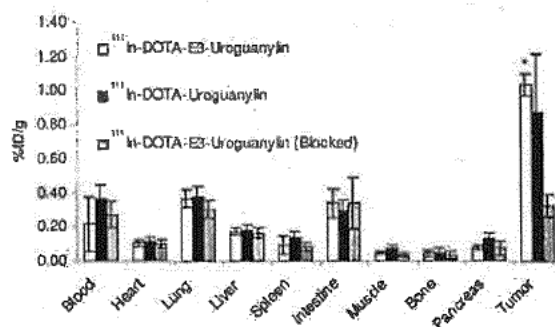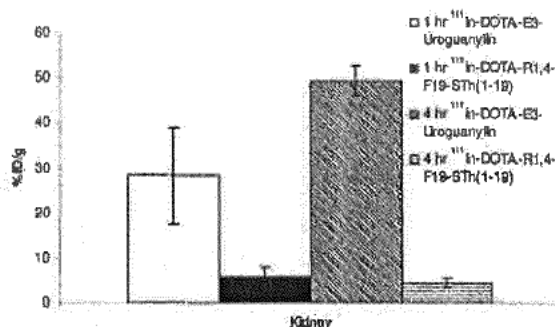

Figure 5. Kidney uptake of ^{111}In-DOTA-E[3]-uroguanylin at 1 and 4 hours post injection compared with kidney uptake of ^{111}In-DOTA-R[1,4],F[19]-STh(1-19)[13] at the same time points.

uroguanylin kidney uptake at this timepoint was greater than 10-fold higher (Figure 5). This high kidney uptake was blocked by co-injection of excess unlabeled E[3]-uroguanylin, decreasing from 28.3 ± 10.6 % ID/g to 14.9 ± 3.0 % ID at 1 hour *p.i.* Despite this higher kidney uptake however, *in vivo* SPECT/CT imaging clearly showed specific uptake of ^{111}In-DOTA-uroguanylin in T84 tumor xenografts (Figure 6). The tumor:kidney ratio of ^{111}In-DOTA-E[3]-uroguanylin is lower than previously observed for ^{111}In-labeled STh analogs (13-15). However, uptake in other nontarget tissues is also low, demonstrating the utility of radiolabeled uroguanylin peptide analogs for the localization of GC-C-expressing cells *in vivo*.

Discussion

Research into the development of peptide ligands targeting the GC-C receptor has resulted in the generation of numerous analogs with a diverse array of incorporated structural alterations. The development of GC-C targeted
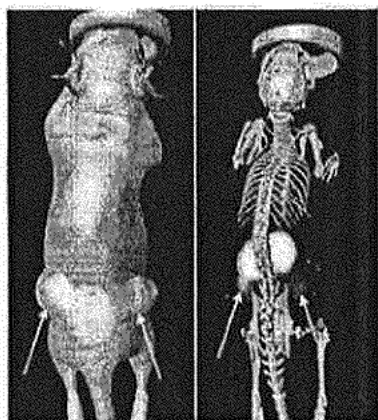
Figure 6. *SPECT/CT image of a SCID mouse bearing bilateral hind flank T84 human colorectal cancer tumor xenografts 1 hour p.i. of 220 μCi* ^{111}In-DOTA-uroguanylin. *Arrows indicate locations of tumors.*

radiopharmaceutical agents has until now centered on the use of tri-disulfide analogs of the heat-stable enterotoxin molecule, due to their having the highest affinity known for the GC-C receptor. In this work, we have compared the properties of such a peptide with those of structurally related uroguanylin peptides. Uroguanylin peptides are the endogenous ligands for the GC-C receptor, have lower affinity for the GC-C receptor, and lack one of the three disulfide bonds present in heat-stable enterotoxin peptides, thereby simplifying their chemical synthesis. Comparison of such peptides *in vitro* and *in vivo* makes possible the analysis of the effects of small variations in receptor binding affinities on tumor localization, and could also lead to the imaging of GC-C *in vivo* with a structurally simpler class of peptide ligands.

In this study, we have synthesized two modified analogs of uroguanylin, and compared their *in vitro* and *in vivo* properties with previously characterized *E. coli* heat-stable enterotoxin analogs possessing an array of linker sequences to *N*-terminal DOTA moieties. Each uroguanylin peptide also possessed an *N*-terminal DOTA chelating moiety, which is capable of complexing a wide range of trivalent imaging and therapeutic radionuclides, including $^{90}Y^{+3}$, $^{111}In^{+3}$, $^{149}Pm^{+3}$, $^{153}Sm^{+3}$, $^{166}Ho^{+3}$, and $^{177}Lu^{+3}$. Each DOTA-peptide was synthesized and purified by C18 RP-HPLC. Both DOTA-uroguanylin and DOTA-E³-uroguanylin were shown to have lower affinity for the GC-C receptor than previously characterized DOTA-STh peptides (13-15). For example, DOTA-uroguanylin showed approximately a 10-fold lower affinity than DOTA-R^{1,4},F^{19}-STh(1-19) in an *in vitro* competitive receptor binding assay. A conservative D3E substitution in wild-type human uroguanylin was shown to increase the affinity of the peptide for GC-C three- to four-fold, resulting in a uroguanylin-based imaging probe with

affinity for GC-C only two- to three-fold lower than that of full-length STh analogs (13-15).

Differences in hydrophobicity between uroguanylin and STh peptides did little to alter the pharmacokinetic behavior of the compounds *in vivo* with respect to parameters such as hepatic excretion. *In vivo*, ^{111}In-DOTA-labeled uroguanylin peptides cleared rapidly from the bloodstream *via* the renal/urinary route, with >83% of injected activity excreted into urine at 1 hour *p.i.* Both uroguanylin analogs however had lower urinary excretion and higher retention in kidney than ^{111}In-labeled STh peptides. Although DOTA-E³-uroguanylin demonstrated significantly higher binding affinity than DOTA-uroguanylin *in vitro*, this change did not result in significantly ($p<0.05$) increased tumor-specific uptake (Figure 4, Table I). At 1 hour *p.i.*, the tumor specificity of ^{111}In-DOTA-E³-uroguanylin was demonstrated by a 69% drop in tumor specific uptake upon coinjection of a blocking dose of unlabeled uroguanylin peptide (Figure 4). Surprisingly, ^{111}In-DOTA-E³-uroguanylin also demonstrated a high degree of uptake in kidney (Figure 5). The high kidney uptake observed at 1 hour *p.i.* (28.3±10.6 % ID) increased even further at 4 hours *p.i.* to 49.4±3.2 % ID, a value more than 10-fold higher than was observed previously for ^{111}In-DOTA-STh peptides at 4 hours *p.i.* (13, 14).

Comparable uptake in kidney has never previously been observed for labeled heat-stable enterotoxin analogs, and suggests the possibility of a novel uroguanylin receptor existing in kidney that can discriminate between uroguanylin and heat-stable enterotoxin ligands. Several experimental findings have contributed to the belief that a receptor for uroguanylin family peptides distinct from the well-characterized GC-C receptor exists. First, induction of natriuresis and kaliuresis by peptides in the uroguanylin family is observed in kidneys of GC-C knockout mice (24). Second, cellular responses to uroguanylin in immortalized human kidney epithelial (IHKE-1) cells were detected in whole cell patch clamp experiments that were distinguishable from responses to an STh peptide (25), suggesting involvement of an unknown pertussis toxin-sensitive G protein in binding of uroguanylin in kidney cells. Third, uroguanylin knockout mice demonstrated a decrease in Na$^+$ excretion following oral salt loads when compared to wild-type controls, while GC-C knockout mice demonstrated no such impairment (26). In this study, kidney uptake of ^{111}In-DOTA-E³-Uroguanylin at 1 hour *p.i.* was reduced 47% by coinjection of 70 μg unlabeled E³-Uroguanylin. However, *in vitro* binding studies utilizing partially purified kidney membranes demonstrated no specific binding of ^{111}In-DOTA-E³-uroguanylin (Data not shown). Therefore, the question of whether the increased kidney uptake of uroguanylin peptides observed here is due to an as yet uncharacterized uroguanylin-specific receptor in kidney, or alternatively is due to a structural property of the uroguanylin peptide such as its acidic *N*-terminus, remains to be determined.

DOCKET ALARM

Explore Litigation Insights

Docket Alarm provides insights to develop a more informed litigation strategy and the peace of mind of knowing you're on top of things.

Real-Time Litigation Alerts

Keep your litigation team up-to-date with **real-time alerts** and advanced team management tools built for the enterprise, all while greatly reducing PACER spend.

Our comprehensive service means we can handle Federal, State, and Administrative courts across the country.

Advanced Docket Research

With over 230 million records, Docket Alarm's cloud-native docket research platform finds what other services can't. Coverage includes Federal, State, plus PTAB, TTAB, ITC and NLRB decisions, all in one place.

Identify arguments that have been successful in the past with full text, pinpoint searching. Link to case law cited within any court document via Fastcase.

Analytics At Your Fingertips

Learn what happened the last time a particular judge, opposing counsel or company faced cases similar to yours.

Advanced out-of-the-box PTAB and TTAB analytics are always at your fingertips.

API

Docket Alarm offers a powerful API (application programming interface) to developers that want to integrate case filings into their apps.

LAW FIRMS

Build custom dashboards for your attorneys and clients with live data direct from the court.

Automate many repetitive legal tasks like conflict checks, document management, and marketing.

FINANCIAL INSTITUTIONS

Litigation and bankruptcy checks for companies and debtors.

E-DISCOVERY AND LEGAL VENDORS

Sync your system to PACER to automate legal marketing.